Nonlinear Relation Between $\dot{V}_{max}$ and I_{Na} in Canine Cardiac Purkinje Cells

Michael F. Sheets, Dorothy A. Hanck, and Harry A. Fozzard

We studied the relation of the maximal upstroke velocity ($\dot{V}_{max}$) of action potentials to the peak sodium current (I_{Na}) under voltage clamp in single, internally perfused, canine cardiac Purkinje cells under conditions that ensured membrane action potentials due only to I_{Na}. Three different methods of altering sodium channel availability were investigated: voltage-dependent inactivation, tetrodotoxin (TTX) block, and use-dependent block by quinidine. Under all three conditions, the relation of $\dot{V}_{max}$ to I_{Na} was nonlinear, and no relation was found that would allow prediction of I_{Na} results from $\dot{V}_{max}$ measurements. With voltage-dependent inactivation or TTX block, sodium channel availability measured by $\dot{V}_{max}$ was reduced less than availability measured by peak I_{Na}, so that $\dot{V}_{max}$ overestimated sodium channel availability. This overestimation of sodium channel availability by $\dot{V}_{max}$ could be attributed to greater sodium channel mobilization during the slowed action potential upstrokes. The overestimation varied with experimental temperature as a consequence of changes in sodium channel kinetics. $\dot{V}_{max}$ also overestimated sodium channel availability during TTX exposure so that the K_d for TTX block was 4.5 μm from $\dot{V}_{max}$ measurements but only 1.6 μM from I_{Na} measurements. Use-dependent block of I_{Na} by quinidine had a striking voltage-dependent component under voltage clamp that could not be appreciated from action potentials. Consequently, block could be underestimated or overestimated by $\dot{V}_{max}$ measurements. We conclude that $\dot{V}_{max}$ measurements represent a convenient index for I_{Na}, but $\dot{V}_{max}$ is not a reliable method for quantitative studies of sodium channel behavior. (*Circulation Research* 1988;63:386–398)

The maximal upstroke velocity of the cardiac action potential ($\dot{V}_{max}$) has traditionally been used as an index of sodium channel availability.[1] $\dot{V}_{max}$, rather than direct measurement of sodium current (I_{Na}), has continued to be used because adequate voltage clamp of I_{Na} has been difficult to achieve in heart cells. While important concepts of the interaction of antiarrhythmic drugs with the sodium channel have been developed using $\dot{V}_{max}$,[2] uncertainty about its quantitative relation to I_{Na} has cast doubt on these concepts.[3–5]

Examination of the relation between $\dot{V}_{max}$ and I_{Na} by I. Cohen et al,[4] using a modified Hodgkin-Huxley model for nerve ionic currents, suggested the requirements necessary for a linear relation. These include longitudinal uniformity of the action potential (i.e., membrane action potential) and the absence of other ionic currents during the upstroke. These requirements are difficult to achieve in the heart, and only one experimental comparison of $\dot{V}_{max}$ and I_{Na} has been published. In shortened strands of rabbit cardiac Purkinje fibers, C. Cohen et al[5] found $\dot{V}_{max}$ and I_{Na} to have a markedly nonlinear relation. However their conclusions have been criticized[6,7] because of possible overlap of I_{Na} with other ionic currents and the experimental conditions of low extracellular Na^+ concentrations, partial inactivation of I_{Na} by membrane depolarization, and experimental temperatures of 17.5° C, all of which they used to control the membrane potential during peak I_{Na}.

We have studied the relation of $\dot{V}_{max}$ to I_{Na} in a single, internally perfused, canine cardiac Purkinje cell preparation that ensured a membrane action potential, isolated I_{Na} from potassium and calcium currents, and permitted use of more physiological Na^+ gradients at warmer experimental temperatures. Although these conditions should favor a linear relation of $\dot{V}_{max}$ to I_{Na}, we found $\dot{V}_{max}$ to have a nonlinear relation to I_{Na} under all experimental

From the Cardiac Electrophysiology Laboratory, Departments of Medicine and the Pharmacological and Physiological Sciences, The University of Chicago, Chicago, Illinois, and The Reingold ECG Center, Department of Medicine, Northwestern University Medical School, Chicago.

Supported by U.S. Public Health Service grants P01 HL 20592 and K11 HL 01971 (M.F.S.).

This manuscript from The University of Chicago was sent to Matthew Levy, Consulting Editor, for review by expert referees, for editorial decision, and for final disposition.

Address for correspondence: Dr. Harry A. Fozzard, Box 440 Cardiology, University of Chicago, 5841 S. Maryland Ave., Chicago, IL 60637.

Received October 27, 1987; accepted February 23, 1988.

conditions. Use-dependent block of sodium channels by quinidine had a striking voltage-dependent component under voltage clamp that could not be appreciated from action potentials, such that use-dependent block could be underestimated or overestimated by $\dot{V}_{max}$ measurements. When sodium channel kinetics were altered by changing experimental temperature, the shape of the $\dot{V}_{max}$ to I_{Na} relation was also altered. This made it impossible to predict the relation of $\dot{V}_{max}$ to I_{Na} after any intervention that also changed sodium channel kinetics. In addition, the K_d of tetrodotoxin (TTX) block of sodium channels obtained by $\dot{V}_{max}$ measurements was 2.8 times that obtained by I_{Na} measurements. We conclude that caution should be used in interpreting any study of sodium channel properties when $\dot{V}_{max}$ is used as a quantitative index of I_{Na}. Some of these results have been presented in abstract form.[8,9]

Materials and Methods

Cell Preparation

The method for preparing single canine cardiac Purkinje cells has been previously described.[10] Briefly, Purkinje fibers from the hearts of adult mongrel dogs were cut into short segments (2–3 mm) and placed in modified Eagle's minimal essential medium, with 5 mg/ml Cooper type I collagenase for 3–4 hours at 37° C. The digested fibers were washed and incubated in 130 mM K-glutamate, 5.7 mM $MgCl_2$, 0.1 mM EGTA, 5.0 mM glucose, and 5.0 mM HEPES (pH 6.2) for 15 minutes before the fibers were mechanically separated into single cells. The single Purkinje cells were stored in Eagle's minimal essential medium (pH 7.2) and were studied within 12 hours of separation.

Solutions

Solutions were chosen to favor only I_{Na}. Extracellular solutions contained 1.8 mM $CaCl_2$, 1.0 mM $MgCl_2$, 10 mM HEPES (pH 7.2), and either 45 or 120 mM NaCl with 104 or 29 mM CsCl, respectively. The internal perfusate contained 10 mM EGTA, 50 μM Mg-ATP, and 10 mM HEPES (pH 7.2) and either 15 mM NaF with 134 mM CsF or only 149 mM CsF. Junction potentials between the internal and external solutions, measured by the method of Oxford,[11] were less than 0.6 mV and therefore were neglected. Quinidine sulfate was obtained from Sigma Chemical, St. Louis, Missouri, and TTX was obtained from Calbiochem, San Diego, California.

External solution changes were made within 30 seconds by moving the pipette with the Purkinje cell from one bath chamber to another chamber separated by a 10-mm length of Plexiglas. Solution changes were considered complete when the experimental reversal potential equaled the predicted reversal potential (from the Nernst equation) or the current response to a step depolarization stabilized.

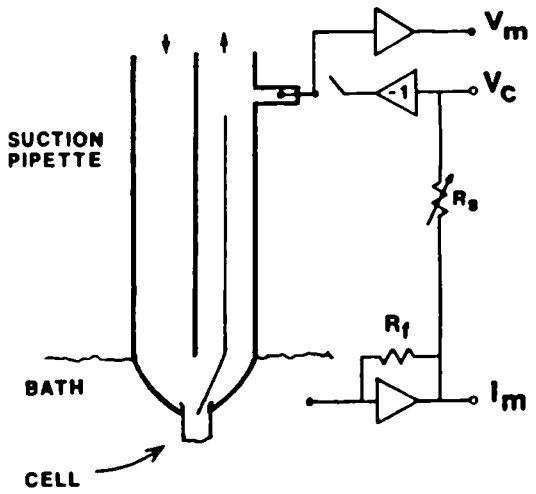

FIGURE 1. *Schematic of the experimental apparatus. See text for discussion.*

Temperature was controlled by a thermoelectric device (TS4, Sensortek, Clifton, New Jersey) that cooled (or heated) the bath solutions and internal solution. Temperature changes could be completed in less than 3 minutes.

Voltage Clamp and Action Potential Recording Technique

A schematic of the apparatus is shown in Figure 1. A large bore (about 25 μm) double-barrelled glass suction pipette was used for both voltage clamp and internal perfusion as previously described.[12] A single cell with normal striation pattern and no membrane blebs was drawn into the aperture until about one third remained outside the pipette. The cell was allowed to seal to the aperture walls, and then the cell segment within the pipette was ruptured by a manipulator-controlled platinum wire to allow access of the pipette solution to the cell interior.

Command voltages were generated by a 16-bit D/A converter (Masscomp 5500 System microcomputer, Westford, Massachusetts) and were presented to the cell through a unity-gain amplifier (OPA27 Burr-Brown, Tucson, Arizona). Currents were measured by a current-to-voltage amplifier (OPA101) with a 5 or 10 MΩ feedback resistor. The response time of the voltage clamp circuitry allowed step changes to settle to within 1% of the final potential in 10 μsec. Capacitive currents were recorded by a 12-bit A/D converter (Masscomp) at 400 kHz. The primary time constant of the membrane capacity current decay (τ_{cap}) after series resistance compensation was usually less than 5 μsec, and the series resistance was approximately 3 Ω-cm.[12] For measurement of I_{Na}, signals were analog filtered with an eight-pole Bessel filter (848 Frequency Devices, Haverhill, Massachusetts) at 50 kHz and digitized at 100 kHz.

To generate action potentials, an electronic relay (Magnecraft, Chicago, Illinois) released the Purkinje cell from voltage clamp distal to the unity-gain

amplifier (Figure 1). The electronic relay required 80–110 μsec to open after an appropriate stimulus. Because the response of the relay was rapid, the release times in the results section have not been corrected for the delay. Action potentials were measured by a high impedance (10^{13} Ω) electrometer (AD515 Analog Devices, Norwood, Massachusetts), analog filtered with an eight-pole Bessel filter at 50 kHz, and digitized at 100 kHz.

Data Analysis

Cell capacitance was measured as the scaled integral of four transient current responses to steps from −150 mV to −190 mV. Integration was performed for 1 msec following the change in voltage; measurements of capacitance were usually constant by 100 μsec. Capacitive decays were fit as one or the sum of two exponentials by a Fourier method.[13] Leak resistance was calculated from currents during voltage clamp steps between −190 mV and −100 mV.

Current recordings were digitally (Gaussian) filtered at 5–12 kHz, depending upon the temperature, and peak I_{Na} was calculated by subtracting the leak current at the end of the step depolarization from the peak transient current. Capacity subtraction was not performed because the short τ_{cap} allowed for clear separation of I_{Na} from I_{cap}. The action potential was also digitally (Gaussian) filtered at 3–20 kHz (depending upon the magnitude of $\dot{V}_{max}$) and then digitally differentiated to obtain dV/dt.

Predicted $\dot{V}_{max}$ was calculated from the equation:

$$\text{Predicted } \dot{V}_{max} = I_{Na}/C_m \quad (1)$$

where C_m is measured as described above, and I_{Na} is the peak inward current during a voltage clamp step from a given conditioning potential to the membrane potential at $\dot{V}_{max}$. I_{Na} was read directly or interpolated from the cell's peak I_{Na}-voltage (I-V) relation measured with full sodium channel availability and scaled by the value from the availability curve for the corresponding conditioning potential. Thus, predicted $\dot{V}_{max}$ represents the value that would be achieved if all the sodium channels that opened at peak I_{Na} during a voltage clamp step to the membrane potential at $\dot{V}_{max}$ also opened at measured $\dot{V}_{max}$.

Data obtained from voltage-dependent inactivation protocols were fit to the Boltzmann distribution equation,

$$[1+\exp((V_c - V_{1/2})/\text{slope})]^{-1} \quad (2)$$

using a modified Gauss-Newton nonlinear least-squares algorithm (NAG, Numerical Algorithms Group, Downers Grove, Illinois) on the Masscomp microcomputer and where V_c was the conditioning membrane potential. Although this equation does not precisely describe the inactivation properties of the cardiac sodium channel,[12] deviations in these experiments were not large enough to prevent use of the equation for comparisons of I_{Na} and $\dot{V}_{max}$ (see Figures 5 and 6).

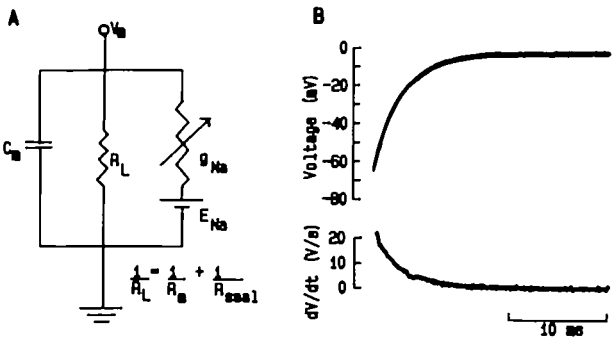

FIGURE 2. Panel A: *Equivalent circuit during action potential measurements. C_m, cell membrane capacitance, and R_L, leak resistance, are measured as described in "Materials and Methods." R_L represents the parallel equivalent resistance of the cell to glass seal resistance (R_{seal}) and the cell membrane resistance when sodium channels are closed (R_m). The active limb is the sodium conductance (g_{Na}) and the electrochemical gradient (E_{Na}).* Panel B: *Passive discharge (upper panel) of C_m through R_L in a Purkinje cell with a C_m of 89 pF and a R_L of 32 MΩ at 17° C (cell 53.01.14). The single exponential fit (τ=2.90 msec) is also plotted. Sodium channels were inactivated by a 500 msec conditioning step to −70 mV, briefly clamped to −65 mV, and then released from voltage clamp. The dV/dt, recorded when Na channels open, is equal to the sum of the dV/dt from the passive limb and the dV/dt from the active limb. Therefore, $\dot{V}_{max}$ due to sodium channel openings equals the recorded $\dot{V}_{max}$ minus the passive dV/dt (that value of passive dV/dt at the membrane potential of $\dot{V}_{max}$). Note that the passive contribution to total dV/dt becomes very small as voltage approaches 0 mV.*

K_d for TTX was calculated from cumulative dose-response data fit to a linearized form of the one-to-one binding relation,

$$(1+[\text{TTX}]/K_d)^{-1} \quad (3)$$

using linear least squares. Grouped data are expressed as mean ± SD except where otherwise noted. Simple and paired *t* tests were performed on an IBM-AT using SAS (Statistical Analysis Systems, Cary, North Carolina). Means of more than two groups were compared using Tukey's Studentized range test.

Results

Equivalent Circuit and Passive Properties

The equivalent circuit for action potential measurements is shown in Figure 2A. The circuit is composed of three limbs; the cell capacitance (C_m), a resistive leak (R_L), and the voltage and time-dependent sodium conductance (g_{Na}). The passive leak resistance (R_L) is the parallel combination of the seal resistance of the cell to the glass (R_{seal}) and the cell membrane resistance when sodium channels are closed (R_m). The methods for measuring C_m and R_L are described in the "Materials and Methods," and their values for the 37 cells included

in this study ranged from 50 to 120 pF and from 10 MΩ to 200 MΩ, respectively. Figure 2B shows the passive membrane potential decay and its dV/dt in a cell when all sodium channels were voltage inactivated. After release from voltage clamp at −65 mV, C_m passively discharged through R_L to the resting membrane potential of 0 mV with a τ of 2.90 msec, very close to the value of 2.85 msec predicted from the measured C_m (89 pF) and R_L (32 MΩ). In five additional cells, we compared the measured passive decay time constant to that predicted from C_m and R_L and found them similar. When sodium channels are open, the measured dV/dt is the sum of dV/dt in the active (g_{Na}) and passive limbs (R_L). Correction of dV/dt for the passive component is possible because passive dV/dt is proportional to the membrane potential and this correction was made when appropriate. However, for most $\dot{V}_{max}$ measurements the contribution of the passive component to measured dV/dt was negligible because the dV/dt from the passive limb was small, especially when the membrane potential approached 0 mV.

Influence of Release Potential on $\dot{V}_{max}$

Before studying the relation of $\dot{V}_{max}$ to I_{Na}, we investigated how the method of eliciting action potentials affected upstroke velocity. Cells were held at −150 mV to remove sodium channel inactivation (i.e., maximize sodium channel availability) and were released from voltage clamp by the electronic relay. Figure 3 (upper) shows the effect of different release potentials on membrane voltage responses (action potentials) from a Purkinje cell perfused with 120 mM Na_o and 15 mM Na_i at 17° C. The cell was clamped to the release potential for 50 μsec prior to release from voltage clamp. After release, the membrane potential passively decayed to the sodium channel threshold (about −70 mV), which caused a rapid upstroke of an action potential with an overshoot to +50 mV (close to the reversal potential of +48 mV predicted by the Nernst equation). Membrane potential then decayed to the resting membrane potential of 0 mV (not shown). When the cell was released from more positive potentials, threshold for I_{Na} was reached sooner, and the rapid upstroke of the action potential occurred earlier. Figure 3 (lower) shows the dV/dt for each action potential upstroke shown in the upper panel. Even though the different release potentials caused the upstrokes to occur at different times, the $\dot{V}_{max}$ values are similar (334 ± 10 V/sec), implying that significant sodium channel inactivation did not occur before the onset of the action potential upstroke. In 12 cells at ≤21° C, maximal $\dot{V}_{max}$ was unaffected by passive decays lasting up to 9 msec but at warmer temperatures of 26–27° C, $\dot{V}_{max}$ was slightly diminished after only 2 msec delay. We were unable to study cells reliably at temperatures greater than 27° C because I_{Na} kinetics became so rapid that the method of initiating action potentials influenced $\dot{V}_{max}$.

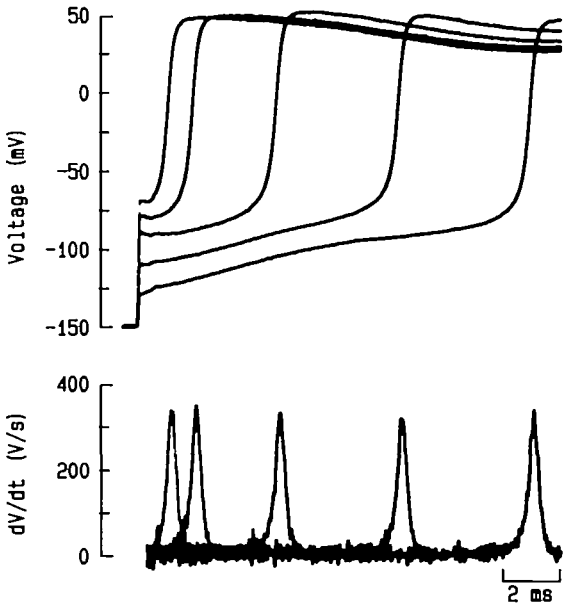

FIGURE 3. *Membrane voltage responses (action potentials) and their dV/dt after release from voltage clamp. Upper panel shows the action potentials after the cell was clamped at −150 mV, stepped to −130, −110, −90, −80, and −70 mV for 50 μsec and then released from voltage clamp. Note the slow decay of membrane potential until I_{Na} threshold was reached at about −70 mV. The rapid upstroke achieved an overshoot of +50 mV. Lower panel shows the dV/dt for each of the action potentials. $\dot{V}_{max}$ are similar even though the upstroke of the action potential from a release potential of −130 mV occurred almost 9 msec later than from a release potential of −70 mV. Purkinje cell (34.01.05) was perfused with 120 mM Na_o and 15 mM Na_i at 17° C. Data were digitally filtered at 8 KHz.*

Influence of the Duration of the Release Potential on $\dot{V}_{max}$

We also investigated the effect on $\dot{V}_{max}$ of the length of time the cell was held at the release potential. Figure 4A (upper) shows the action potentials elicited in a Purkinje cell with 45 mM Na_o and 0 mM Na_i at 26° C. The cell was stepped from −150 mV to −65 mV for 100, 200, 300, or 400 μsec and then released from voltage clamp. Figure 4A (lower) shows the dV/dt for each upstroke of the four action potentials. With release potential durations of 100 and 200 μsec, the magnitudes of $\dot{V}_{max}$ were similar, 495 and 500 V/sec, respectively, while with release durations of 300 and 400 μsec, $\dot{V}_{max}$ increased to 543 and 663 V/sec, respectively. Figure 4B shows the current record from a voltage clamp step to −65 mV on the same time base as Figure 4A. Significant I_{Na} developed after 200 μsec and reached a peak of −65 nA at about 700 μsec, concomitant with the increase in $\dot{V}_{max}$. If the release from voltage clamp had occurred at peak I_{Na}, then $\dot{V}_{max}$ would have been 1,250 V/sec. The release protocol was performed in seven cells at temperatures between 7° C and 26° C and $\dot{V}_{max}$ was independent of the release potential duration so long as significant I_{Na} did not develop

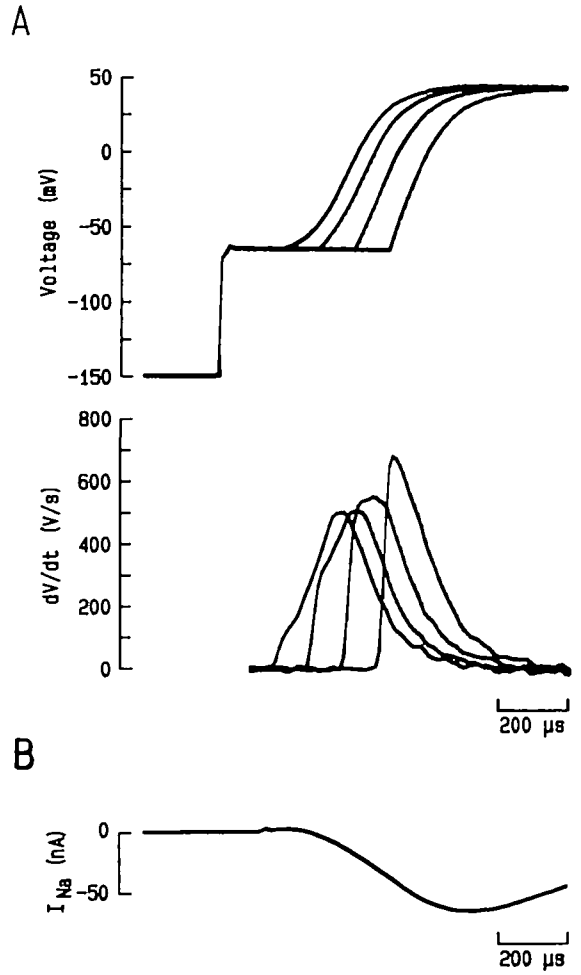

FIGURE 4. Panel A: *Action potentials and their dV/dt when the cell was held at the release potential of −65 mV for 100, 200, 300, and 400 µsec before release from voltage clamp. The action potential upstroke (upper panel) occurred earlier and was faster as the cell was held longer at the release potential before being released from voltage clamp. Middle panel shows dV/dt for each of the four action potentials. With release potential durations of 100 and 200 µsec the magnitudes of $\dot{V}_{max}$ are similar, 495 and 500 V/sec, respectively, while with release durations of 300 and 400 µsec, $\dot{V}_{max}$ increased to 543 and 663 V/sec, respectively.* Panel B: *Capacity and leak corrected I_{Na} from a voltage clamp step from −150 mV to −65 mV. Significant I_{Na} developed after 200 µsec and reached a peak of −65 nA at about 700 µsec. Purkinje cell (53.01.20) was perfused with 45 mM Na_o and 0 mM Na_i at 26° C. Data are digitally filtered at 12 kHz.*

prior to release. To ensure that the stimulation protocol did not influence $\dot{V}_{max}$, Purkinje cells were released near threshold potential with release potential durations of ≤100 µsec.

Comparison of $\dot{V}_{max}$ to I_{Na} Using Voltage-Dependent Inactivation

Voltage-dependent inactivation was used to alter sodium channel availability for both I_{Na} and $\dot{V}_{max}$ measurements. The protocol used for I_{Na} measurements is illustrated in the inset to Figure 5. The cell was held at conditioning potentials between −150 mV and −70 mV for 500 msec and then stepped to a constant test potential on the positive slope of the I-V relation. Peak I_{Na} was normalized to the largest peak current after correction for the small leak current at the end of the 25 msec test step. Figure 5 shows I_{Na} recorded in a typical cell at 17° C with 45 mM Na_o and 0 mM Na_i (Panel A) and the plot of fractional I_{Na} versus membrane conditioning potential (Panel B). The solid curve is the fit to the Boltzmann distribution equation (Equation 2) where $V_{1/2} = -106$ mV and the slope = 5.8.

A similar voltage protocol was used to vary sodium channel availability for $\dot{V}_{max}$ determinations. After 500-msec conditioning steps, action potentials were elicited by stepping to a potential near I_{Na} threshold for 50–100 µsec before releasing the cell from voltage clamp. Figure 6A shows action potential upstrokes and their dV/dt from the same Purkinje cell in Figure 5. When the conditioning potential was −150 mV, the membrane depolarization was rapid with an overshoot to +54 mV and a $\dot{V}_{max}$ of 358 V/sec. However, as more sodium channels were inactivated at more positive conditioning potentials, the overshoot diminished, and $\dot{V}_{max}$ declined. With all sodium channels inactivated, the membrane potential decayed exponentially to 0 mV after release from voltage clamp. Figure 6B shows the plot of fractional $\dot{V}_{max}$ versus membrane conditioning potential and the fit to the Boltzmann distribution equation (Equation 2). $V_{1/2}$ from $\dot{V}_{max}$ measurements was −103 mV, 3 mV more positive than $V_{1/2}$ based upon I_{Na} measurements.

Figure 7 shows the $\dot{V}_{max}$ measurements from Figure 6B plotted against the I_{Na} measurements from Figure 5B. Also plotted are the fits to the Boltzmann distribution equation and the line of identity. When the plots from Figures 5B and 6B are superimposed (Figure 7 inset), they appear close together. However, the plot of the $\dot{V}_{max}$ against I_{Na} emphasizes that $\dot{V}_{max}$ overestimates sodium channel availability. For example, when I_{Na} showed sodium channel availability to be 0.10, $\dot{V}_{max}$ measurements showed sodium channel availability to be almost 0.20, an overestimate of nearly 100%. The $\dot{V}_{max}$ to I_{Na} relation was similar in all experiments at 17–20° C (see Figure 9).

We have previously reported hyperpolarizing shifts in sodium channel availability and activation during the course of an experiment.[12] To avoid any effect of such a shift on the comparison between I_{Na} and $\dot{V}_{max}$, all voltage-dependent inactivation protocols alternated five cycles of I_{Na} measurements with five cycles of $\dot{V}_{max}$ measurements for a total of 30 cycles during each 30-second protocol. The experimental results were not different if the protocol started first with action potentials or first with voltage clamp steps. This is expected since the half-point of the availability curve shifted to more

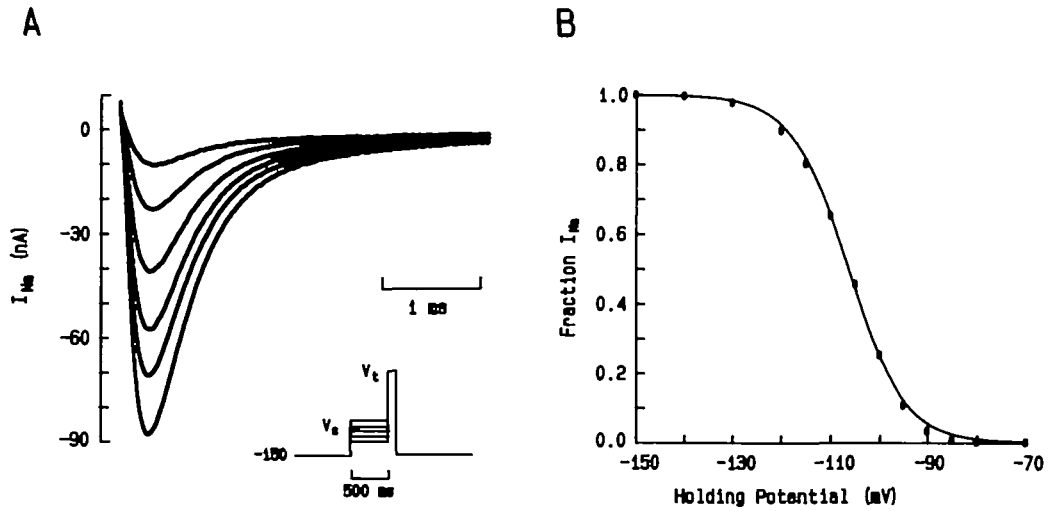

FIGURE 5. *I_{Na} availability assessed from step depolarizations to 0 mV (V_t) after 500 msec conditioning steps to various V_c (see inset).* Panel A: *Current responses to conditioning potentials of −150, −115, −110, −105, −100, and −95 mV.* Panel B: *Fractional I_{Na} normalized to the largest value (−86 nA) vs. conditioning potential. The solid line is the fit to Equation 2 ($V_{1/2}$ −106 mV, slope 5.8). Purkinje cell (53.01.14) perfused with 45 mM Na_o and 0 mM Na_i at 17° C. Current digitally filtered at 5 KHz.*

negative potentials at a relatively slow rate of -0.6 ± 0.2 mV/min ($n = 5$). In addition, in five cells we compared the $\dot{V}_{max}$ to I_{Na} relation early and late in the typical 45-minute "life" of the cell and found the $\dot{V}_{max}$ to I_{Na} relation unaltered.

Effect of Extracellular Na^+

To assess the effect of Na_o upon the relation of $\dot{V}_{max}$ to I_{Na}, the results from voltage-dependent inactivation protocols in seven Purkinje cells with 120 mM Na_o were compared with seven cells with 45 mM Na_o at experimental temperatures of 18–20° C (Figure 8). Even though peak $\dot{V}_{max}$ in 45 mM Na_o (255 ± 45 V/sec) was lower than that in 120 mM Na_o (386 ± 71 V/sec), the differences in the Boltzmann parameters between I_{Na} and $\dot{V}_{max}$ at the two concentrations were not significantly different. The half-point for $\dot{V}_{max}$ was more positive than the I_{Na}

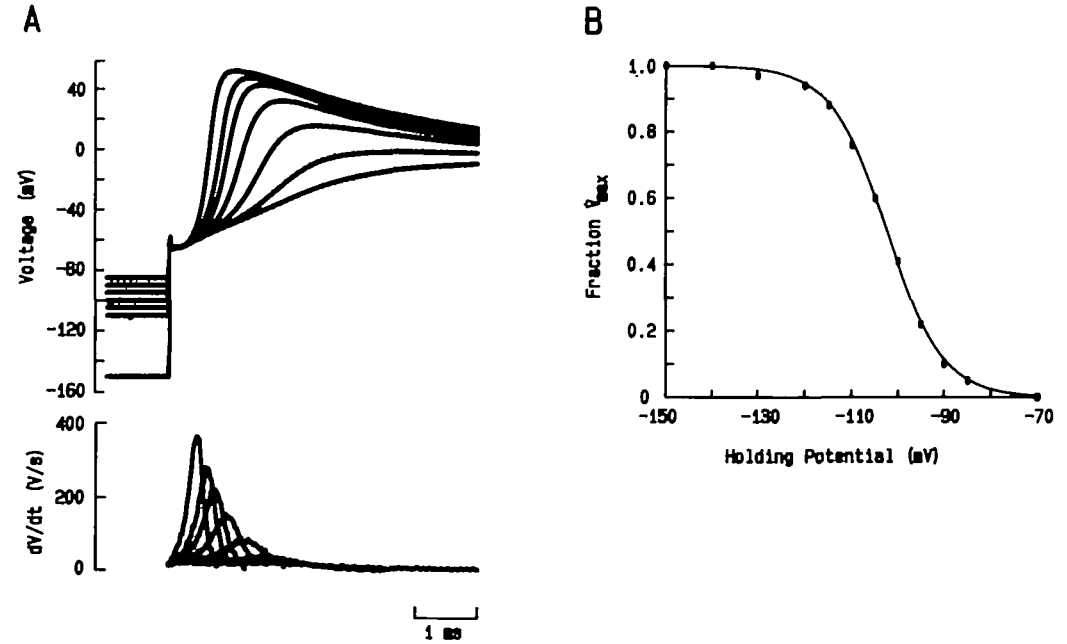

FIGURE 6. *Action potentials after a 500 msec conditioning pulse to various V_c in the same Purkinje cell shown in Figure 5.* Panel A: *Action potentials (top) and their dV/dt (bottom) after conditioning for 500 msec at −150, −110, −105, −100, −95, −90, and −85 mV and then stepping to −65 mV for 50 μsec before releasing the cell from voltage clamp.* Panel B: *Fractional $\dot{V}_{max}$ normalized to the largest value (360 V/sec) vs. conditioning potential. The solid line is the fit to Equation 2 ($V_{1/2}$ −103 mV, slope 5.7).*

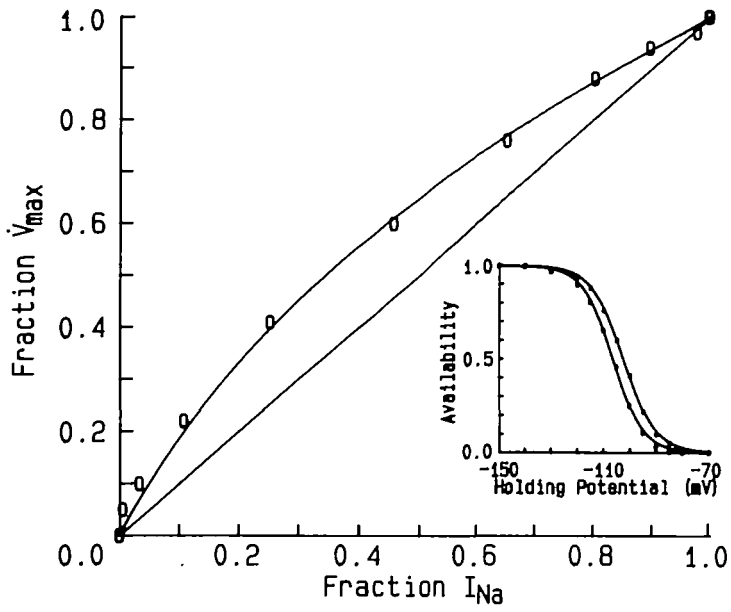

FIGURE 7. *Fractional I_{Na} and fractional $\dot{V}_{max}$ plotted against each other at corresponding conditioning potentials from Figures 5 and 6. The curved line is the Boltzmann distribution fits and the straight line is the line of identity. The insert shows the plots from Figures 5B and 6B superimposed. Normalized I_{Na} is to the left of normalized $\dot{V}_{max}$.*

half-point by 3.4±0.7 mV in 45 mM Na_o and by 4.1±0.8 mV in 120 Na_o. The difference in slope was −0.2±0.5 in 45 mM Na_o and −0.3±0.3 in 120 mM Na_o. Thus, the nonlinearity of $\dot{V}_{max}$ to I_{Na} appears not to be a function of extracellular Na^+.

Effect of Temperature

To investigate the effect of changes in sodium channel kinetics on the relation of $\dot{V}_{max}$ to I_{Na}, we varied the experimental temperature from 7° to 27° C. Voltage-dependent inactivation protocols were used as described above, and each of the data sets for I_{Na} and $\dot{V}_{max}$ was fitted to Equation 2 to obtain $V_{1/2}$ and slope values. The results in a cell studied at two different temperatures are shown in Figure 9A. At 8° C, the relation between I_{Na} and $\dot{V}_{max}$ was more nonlinear than at 26° C. Figure 9B shows summary data from nine cells studied at three temperature ranges (7–10° C, 17–20° C, and 26–27° C) and compares the $V_{1/2}$ and slopes from fits to Equation 2. The largest differences between $V_{1/2}$ and slopes occurred at the coldest temperature, 7–10° C. At 26–27° C, where the relation between $\dot{V}_{max}$ and I_{Na} became less nonlinear, the difference in $V_{1/2}$ decreased, and the slope from $\dot{V}_{max}$ values became steeper than that from I_{Na}. A paired t test showed the low temperature data to be significantly different from the high temperature group at $p<0.05$.

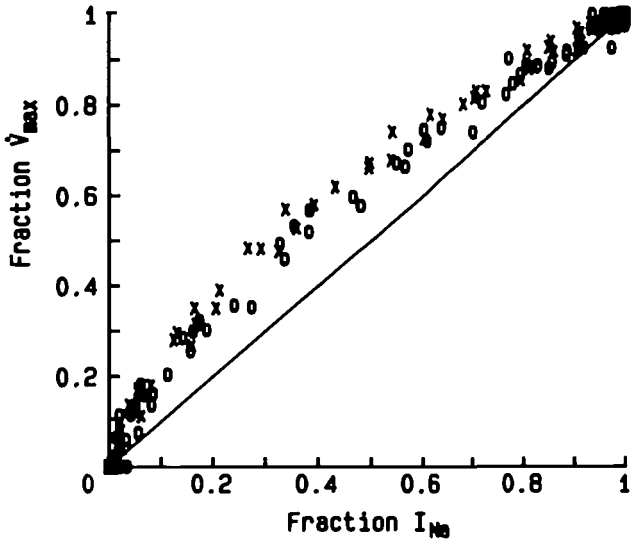

FIGURE 8. *Effect of electrochemical driving force on the relation of I_{Na} to $\dot{V}_{max}$ in Purkinje cells perfused with either 120 mM Na_o (×, n=7) or 45 mM Na_o (○, n=7), and 15 mM Na_i at 18–20° C. Fractional $\dot{V}_{max}$ was plotted against fractional I_{Na} for the corresponding conditioning membrane potentials.*

We considered whether these temperature-dependent differences could be attributed to changes in the membrane potential at $\dot{V}_{max}$ and therefore to changes in the electrochemical driving force. Figure 10 shows the membrane potential at the time of $\dot{V}_{max}$ for three cells that were studied in each of the three temperature ranges. Within each data set, as $\dot{V}_{max}$ became smaller, the membrane potential at $\dot{V}_{max}$ became more negative, which increased the electrochemical driving force and helped contribute to the nonlinearity of $\dot{V}_{max}$ to I_{Na}. Near 8° C, the change in membrane potential at $\dot{V}_{max}$ was nearly 20 mV (from +10 mV to −10 mV), while at 26° C, the change was almost 40 mV (from −10 mV to −50 mV). Even though the greatest increase in electrochemical driving force occurred at 26° C, the nonlinearity of I_{Na} to $\dot{V}_{max}$ was the least, suggesting that changes in the electrochemical driving force are not the primary cause for the nonlinear relation. The membrane potential at maximal $\dot{V}_{max}$ was the most positive at the coldest temperature (8.0±3.6 mV, $n=3$) and the most negative at 26–27° C (−10.0±4.3 mV, $n=3$), presumably because of faster activation of I_{Na} at warmer temperatures. An analysis of

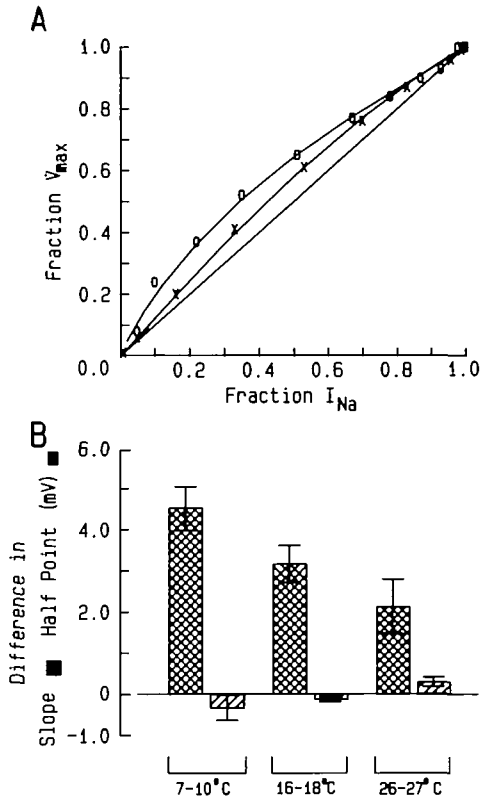

FIGURE 9. *Effect of experimental temperature on the relation of I_{Na} to $\dot{V}_{max}$.* Panel A: *$\dot{V}_{max}$ to I_{Na} relation in a Purkinje cell at 8° C* (○) and 26° C (×). Cell 53.01 with 45 mM Na_o and 0 mM Na_i. Solid lines are fits to Equation 2. Panel B: *Grouped data from nine cells studied in three temperature ranges. Each group includes data from five different cells. The cross-hatched bars represent the mean differences (±SEM) in $V_{1/2}$ from the Boltzmann fits for I_{Na} and $\dot{V}_{max}$. $V_{1/2}$ from $\dot{V}_{max}$ is more positive than $V_{1/2}$ from I_{Na} by the millivolts indicated. The single-hatched bars represent the mean differences (±SEM) in the slope of the Boltzmann fits. A negative value indicates that the slope is less steep for $\dot{V}_{max}$ than for I_{Na}.*

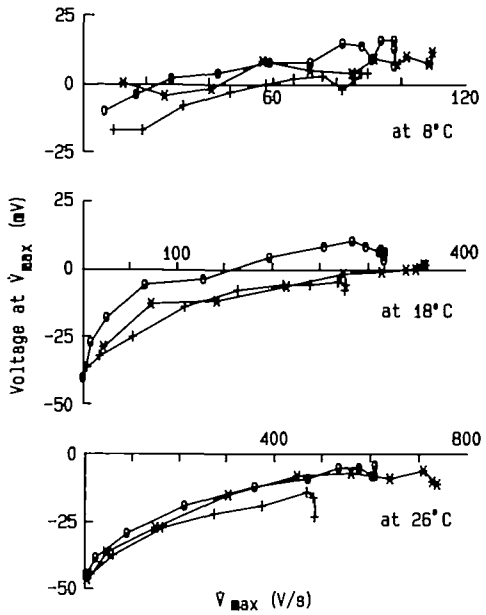

FIGURE 10. *Membrane potential at $\dot{V}_{max}$. Voltage-dependent inactivation protocols were used to vary sodium channel availability. Data are shown for three cells studied at each of the three temperatures in Figure 9: 53.01 (*), 53.02 (+), 53.03 (○).*

grouped data revealed these differences to be significant at $p<0.01$.

The relation of I_{Na} to $\dot{V}_{max}$ varied as a function of experimental temperature probably because of changes in sodium channel kinetics. The cell in Figure 9A at 7° C had a maximal $\dot{V}_{max}$ of 110 V/sec and at 26° C maximal $\dot{V}_{max}$ increased to 740 V/sec (a 6.7-fold increase). Peak I_{Na} (measured at 0 mV) increased from −47 nA to −113 nA (a 2.4-fold increase) over the same temperature range. Similar increases for $\dot{V}_{max}$ and I_{Na} were found for all three cells in Figure 10. If $\dot{V}_{max}$ and I_{Na} measurements reflected the same kinetic process, then their temperature dependence should be similar. However, they are markedly different, because sodium channels are mobilized differently by action potential upstrokes than by voltage-clamp step depolarizations. Consequently, changes in sodium channel kinetics have different effects on I_{Na} and $\dot{V}_{max}$.

To evaluate further the effect of temperature on the relation of $\dot{V}_{max}$ to I_{Na}, we compared the measured $\dot{V}_{max}$ with the predicted $\dot{V}_{max}$ (see "Materials and Methods"). The ratio of measured $\dot{V}_{max}$ to predicted $\dot{V}_{max}$ represents the fraction of sodium channels that actually opened compared with the sodium channels available to open as predicted from voltage clamp. Figure 11 shows the results from the same cell shown in Figure 9A. The fraction of channels that opened at $\dot{V}_{max}$ was 0.25 at 8° C from a conditioning potential of −150 mV and the fraction remained constant until a conditioning potential of −110 mV. As sodium channels inactivated at more positive conditioning potentials with a resultant decrease in $\dot{V}_{max}$, the fraction of sodium channels that opened increased to 0.42 (nearly a 70% increase). At 18° C the fraction of sodium channels opening from a conditioning potential of −150 mV was 0.38, but following a conditioning potential of −90 mV the fraction increased to 0.57, a 56% increase. A similar relation was found in all seven cells in the two low temperature ranges. This increase in fraction of sodium channels opening as $\dot{V}_{max}$ declines appears to be the most important cause for the nonlinearity between I_{Na} and $\dot{V}_{max}$. In contrast at 26° C, where the nonlinearity is less, the fraction of sodium channels opening initially increased but then decreased, probably because significant sodium channel inactivation occurred during the slowed upstroke velocities of the action potentials associated with the more positive conditioning potentials. This decrease in the fraction of channel openings at 26° C was noted in two of four

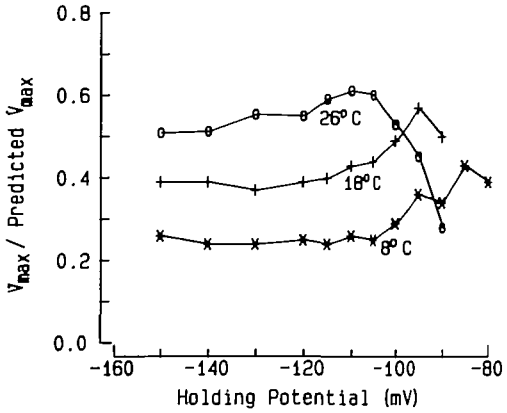

FIGURE 11. *Ratio of measured $\dot{V}_{max}$ to predicted $\dot{V}_{max}$ as a function of holding potential. Cell was voltage inactivated at each of the holding potentials. See text for details. Cell 53.01.*

cells. In the third cell, the fraction of channel openings increased as $\dot{V}_{max}$ decreased and its $\dot{V}_{max}$ to I_{Na} relation was very nonlinear with the difference in $V_{1/2}$ between I_{Na} and $\dot{V}_{max}$ of 2.7 mV. In the fourth cell, where the fraction remained constant, the $\dot{V}_{max}$ to I_{Na} relation was nearly linear with a difference in $V_{1/2}$ of only 0.6 mV.

For nine cells studied, the mean fraction of sodium channels opening following a conditioning potential of −150 mV was 0.21 (±0.05, $n=5$) at 7–10° C, 0.36 (±0.10, $n=5$) at 16–18° C, and 0.52 (±0.01, $n=4$) at 26–27° C; all were significantly different from each other at $p<0.01$.

Comparison of $\dot{V}_{max}$ to I_{Na} Using Tetrodotoxin

We also varied the availability of sodium channels using TTX and compared $\dot{V}_{max}$ with I_{Na} in estimating tonic sodium channel block. TTX in concentrations of 0.5 to 10 μM was applied extracellularly to Purkinje cells with 120 mM Na_o and 15 mM Na_i at 19° C. The voltage protocol remained constant throughout these experiments with a holding membrane potential of −150 mV and a stimulation frequency of 0.2 Hz. After exposure to TTX for at least 30 seconds, cells were either voltage clamped to 0 mV for 25 msec to record peak I_{Na}, or released from clamp to record an action potential. Both I_{Na} and $\dot{V}_{max}$ measurements were normalized to the control values at the beginning of the experiment in the absence of TTX. Figure 12 shows normalized I_{Na} and $\dot{V}_{max}$ versus TTX concentration for four Purkinje cells, with the solid lines representing the least-squares fit to the one-to-one binding curve (Equation 3). Note that $\dot{V}_{max}$ again overestimated sodium channel availability. The $\dot{V}_{max}$ binding curve gave a K_d for TTX of 4.5 μM and was 2.8 times greater than the K_d of 1.6 μM from the I_{Na} binding curve.

Errors in estimation of K_d might be expected from dose response relations obtained cumulatively. Because the one-to-one binding equation contains

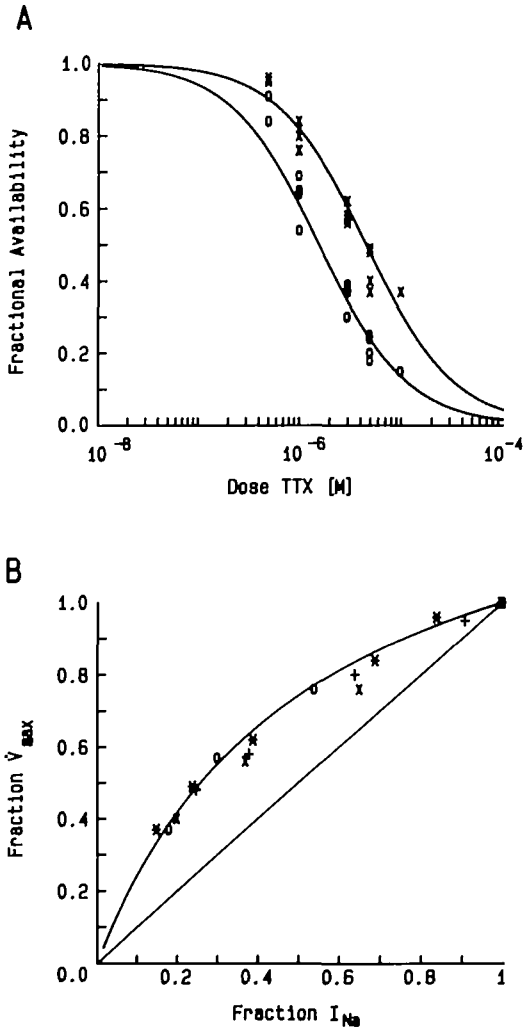

FIGURE 12. *Tonic block by TTX in four Purkinje cells perfused with 120 mM Na_o and 15 mM Na_i at 19° C.* Panel A: *Dose-response data show fractional I_{Na} (○) to the left of fractional $\dot{V}_{max}$ (×). The solid curves are fits to the one-to-one binding equation (Equation 3). The K_d from I_{Na} data was 1.6 μM while that from $\dot{V}_{max}$ data was 4.5 μM.* Panel B: *Fractional I_{Na} and fractional $\dot{V}_{max}$ plotted against each other at corresponding TTX concentrations. The straight line is the line of identity and curved line is the TTX binding curve for I_{Na} plotted against that for $\dot{V}_{max}$. Both the I_{Na} and $\dot{V}_{max}$ measurements were normalized to their control values at the beginning of the experiment in the absence of TTX. Data from individual cells are identified as 34.03 (○), 34.04 (×), 35.01 (*), and 35.04 (+).*

K_d as the only free parameter, it is possible to estimate K_d from the first dose alone and to compare this K_d with that from the cumulative dose response data. The K_d values estimated from only the first dose of TTX and those estimated from all doses were only slightly different so that the K_d values calculated from $\dot{V}_{max}$ and I_{Na} measurements using the two analysis methods were still different by a factor of 2.4 to 2.8.

Comparison of $\dot{V}_{max}$ and I_{Na} in Assessing Quinidine Block

Because $\dot{V}_{max}$ has frequently been used to investigate the action of use-dependent block of I_{Na} by antiarrhythmic drugs, we studied the relation of $\dot{V}_{max}$ to I_{Na} in the presence of the use-dependent antiarrhythmic drug quinidine at concentrations of 10–20 μM.[14] The response of $\dot{V}_{max}$ and I_{Na} during trains of 28 pulses at 3 Hz with 45 mM Na_o and 15 mM Na_i was studied at 17° C. Peak I_{Na} was recorded during 10 or 100 msec test pulses to −30 mV and to +30 mV from a holding potential of −150 mV, and $\dot{V}_{max}$ was recorded as previously described. For $\dot{V}_{max}$ experiments the cell membrane was clamped back to −150 mV either 10 or 100 msec after release from clamp. At least a 2-minute interval was allowed between pulse trains to permit full recovery from block.

Figure 13A shows the results from one of the four Purkinje cells studied. On the abscissa is the cycle number of the pulse train, and on the ordinate is I_{Na} and $\dot{V}_{max}$, each normalized to the value of the first pulse. Note that $\dot{V}_{max}$ decreased substantially with increasing pulse number and by pulse 27, the magnitude of $\dot{V}_{max}$ decreased by 49%, from 221 V/sec to 113 V/sec. I_{Na} also decreased with increasing pulse number, but the amount of block was dependent upon the membrane test potential. At a test potential of −30 mV, I_{Na} decreased by 34%, but at a test potential of +30 mV, I_{Na} decreased by 68%.

In Figure 13B, normalized $\dot{V}_{max}$ is plotted pulse for pulse against I_{Na}. $\dot{V}_{max}$ overestimated block of I_{Na} that developed at a test potential of −30 mV by about 26%. In contrast, $\dot{V}_{max}$ underestimated block of I_{Na} that developed at a test potential of +30 mV by about 66%. When the test pulse durations for both $\dot{V}_{max}$ and I_{Na} were decreased to 10 msec from 100 msec, the relation of $\dot{V}_{max}$ to peak I_{Na} was qualitatively similar but slightly less nonlinear. Results were similar for all four Purkinje cells studied.

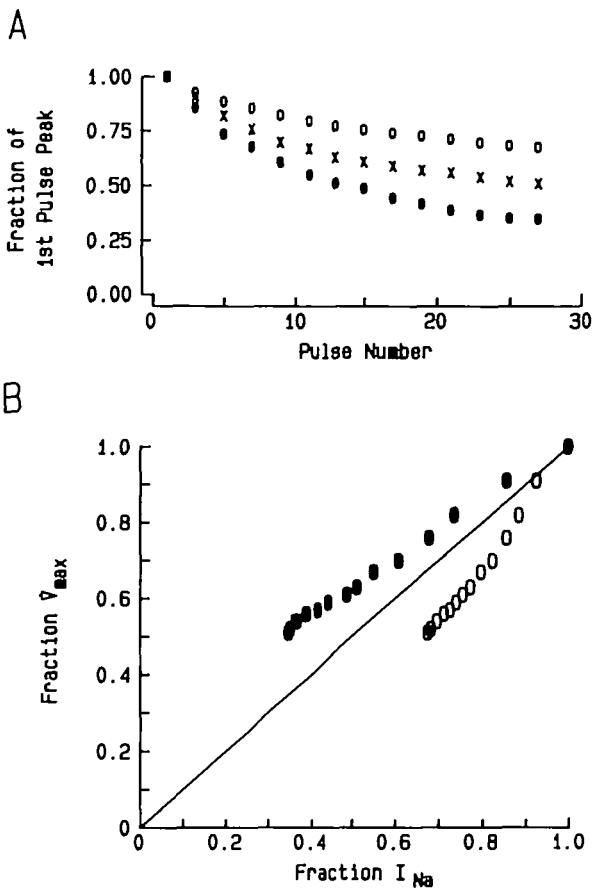

FIGURE 13. *Effect of extracellular quinidine on the relation of I_{Na} to $\dot{V}_{max}$ in trains of 28 pulses at 3 Hz with 45 mM Na_o and 0 mM Na_i at 16.5° C (cell 61.04, 62 pF, R_L 89 MΩ).* Panel A: *The fraction (normalized to the value of the first pulse) of I_{Na} recorded during 100-msec pulses to −30 mV (○) or +30 mV (●) and the fraction of $\dot{V}_{max}$ (×). Peak current at +30 mV fell from −14.4 nA to −5.4 nA (τ=10.9 pulses) and at −30 mV from −56.8 nA to −37.4 nA (τ=13.7 pulses). $\dot{V}_{max}$ fell from 221 V/sec to 113 V/sec (τ=9.7 pulses).* Panel B: *Fractional I_{Na} at −30 mV (○) or +30 Mv (●) plotted against fractional $\dot{V}_{max}$. For clarity only every other pulse is plotted.*

Discussion

The availability of sodium channels was assessed by peak I_{Na} measurement during voltage clamp and by $\dot{V}_{max}$ measurement of action potential upstrokes. Three methods of altering sodium channel availability were used: voltage-dependent inactivation, TTX block, and quinidine use-dependent block. Under each condition, the relation between peak I_{Na} and $\dot{V}_{max}$ was nonlinear and no relation was found that would predict results for I_{Na} from $\dot{V}_{max}$. The discrepancy between the $\dot{V}_{max}$ and I_{Na} measurements could be substantial. Under conditions of extensive sodium channel block or inactivation, the difference was a factor of two or more. For example, the K_d for TTX block differed by a factor of 2.8. We conclude that $\dot{V}_{max}$ measurements cannot be used for quantitative study of sodium channel behavior because the relation of $\dot{V}_{max}$ to I_{Na} varies as a function of sodium channel kinetics even in an experimental preparation that should favor a linear relation.

Experimental Sources of Nonlinearity Between $\dot{V}_{max}$ and I_{Na}

One potential problem in the study of action potential upstrokes is that $\dot{V}_{max}$ can be influenced by the triggering stimulus.[15,16] Using the Hodgkin-Huxley equations for I_{Na}, Walton and Fozzard[17] found that the stimulus affected $\dot{V}_{max}$ because of time-dependent changes in activation and inactivation parameters prior to $\dot{V}_{max}$. This problem could be controlled in their model by requiring the stimulus to achieve a "constant latency" between stimulus and the time of $\dot{V}_{max}$. We carefully examined the effect of the stimulus on action potentials in our experiments and found a range of prerelease poten-

tials and durations for which $\dot{V}_{max}$ was independent of "latency," permitting accurate comparison of $\dot{V}_{max}$ with I_{Na} for experimental temperatures <28° C. The independence of $\dot{V}_{max}$ from latency in our experiments was a consequence of slower channel kinetics at cooler temperatures and the lag before the onset of sodium channel inactivation.[18] While we avoided the problem of stimulus dependence of $\dot{V}_{max}$, latency became important at temperatures ≥28° C, which illustrates the difficulties in using $\dot{V}_{max}$ as an index of I_{Na} in preparations at physiological temperatures.

In multicellular cardiac tissue, where the capacity is in series with a distributed series resistance, the "effective" membrane capacity—the charge that must be displaced by the inward current—is frequency-dependent. Because the "effective" membrane capacitance is less during the rapid upstroke of the normal action potential, it requires less inward current than a slower upstroke causing the relation between inward current and dV/dt to be altered.[19,20] Because single Purkinje cells have no tubules or intercellular clefts, these potential sources for series resistance were avoided in our experiments.

Another potential problem could arise from spacial nonuniformity in membrane potential, which would allow some inward current to flow longitudinally, rather than displacing capacitive charge, and this should alter the $\dot{V}_{max}$ to I_{Na} relation. In our experimental preparation, a membrane action potential was assured[12] so there was no longitudinal current flow. Under most experimental conditions action potentials are made up of several ionic currents that may overlap I_{Na} during the upstroke but the action potential in our studies was due only to I_{Na}. We conclude that any discrepancy between $\dot{V}_{max}$ and I_{Na} in our experiments must have been due to differences between the underlying physiological events.

Reasons for the Nonlinear Relation of $\dot{V}_{max}$ to I_{Na} in Our Studies

With voltage inactivation or TTX block, the availability of sodium channels measured by $\dot{V}_{max}$ was reduced less than the availability measured by peak I_{Na}, so that the $\dot{V}_{max}$ measurements overestimated sodium channel availability relative to peak I_{Na} measurements. Consequently, when upstroke velocity was slow a larger proportion of resting sodium channels contributed to $\dot{V}_{max}$. This is in general agreement with C. Cohen et al[5] who studied voltage clamped rabbit Purkinje fibers. I. Cohen et al,[4] who examined this question using a modified Hodgkin-Huxley model for I_{Na}, predicted that the depolarization rate achieved a maximum so quickly that many channels that would be open at peak I_{Na} do not have time to open at $\dot{V}_{max}$. When sodium channel availability is reduced, depolarization during the action potential is slowed, and greater time is available for sodium channel mobilization. Consequently a larger fraction of the available sodium channels open. We examined this prediction by calculating the predicted $\dot{V}_{max}$ and comparing it with the measured $\dot{V}_{max}$. We found that the ratio of measured to predicted $\dot{V}_{max}$, under conditions when sodium channels were fully available, was 0.21 at 7–10° C, and it increased to 0.52 at 26–27° C. At a constant temperature the ratio also increased as sodium channel availability was reduced. This represents more effective mobilization of sodium channels during the upstroke of the action potential and constitutes a safety factor for conduction because the inward current for conduction (reflected in $\dot{V}_{max}$) did not decrease as much as the number of available sodium channels. Furthermore, the membrane potential at $\dot{V}_{max}$ became more negative when sodium channel availability was reduced. This contributes an additional component to the safety factor because the larger sodium electrochemical driving force allows more current through each open channel at $\dot{V}_{max}$.

The accentuation of the nonlinear relation between the two measures of sodium channel availability at cooler temperatures may be interpreted in terms of the relative rates of channel activation and inactivation if we assume experimental temperature does not alter the quantity of sodium channels. At the coolest temperature, the ratio of measured $\dot{V}_{max}$ to that predicted by peak I_{Na} is half that at 26–27° C, indicating that relatively fewer sodium channels were mobilized during the upstroke of the action potential. The further slowing of the action potential upstroke when availability of sodium channels is reduced by voltage inactivation then permits greater mobilization of channels. Although the dependence of nonlinearity on temperature was predicted by the model calculations of I. Cohen et al,[4] C. Cohen et al[5] did not predict this result because they modeled the upstroke assuming equal temperature dependence for activation and inactivation.

I. Cohen et al[4] also considered the effect of increasing the rate of inactivation relative to activation. Their model predicted an opposite nonlinearity under that condition, with peak I_{Na} predicting more channels available than the $\dot{V}_{max}$ method. This was simply because some channels became inactivated during the slower action potential upstroke. Such inactivation during a slow upstroke was not a significant factor in our experiments because we found $\dot{V}_{max}$ measurements to be independent of the time to $\dot{V}_{max}$. However, at the higher temperature of 26–27° C inactivation was clearly accelerated, and this may have contributed to the decline in the ratio of measured to predicted $\dot{V}_{max}$. It is not possible to predict whether the trend toward less nonlinearity at a warmer temperature would have abolished the nonlinearity at 37° C or would have produced nonlinearity in the opposite direction.

Because $\dot{V}_{max}$ has frequently been used to investigate sodium channel block by antiarrhythmic drugs,[14] we compared $\dot{V}_{max}$ and I_{Na} as measures of use-dependent block by quinidine during pulse trains. Block of I_{Na} by quinidine had a striking voltage-dependent component under voltage clamp with

greater block at +30 mV than at −30 mV. During pulse trains, $\dot{V}_{max}$ also decreased as the action potential upstroke slowed and the overshoot diminished, but the voltage-dependent nature of the block could not be appreciated. Changes in action potential shape during pulse trains, as might occur when plateau currents are altered by quinidine,[21] should influence the interaction of quinidine with sodium channels and cause the relation of $\dot{V}_{max}$ to I_{Na} to be different. With voltage clamp, such voltage dependence can be readily seen as long as more than one test potential is studied, but with action potential experiments, more complicated experimental protocols are required to note voltage dependence.[22]

Role of $\dot{V}_{max}$ Measurements in the Study of I_{Na}

What is the role of $\dot{V}_{max}$ in future studies of sodium channels? Although $\dot{V}_{max}$ accurately reflects the net maximal inward current contributing to the depolarization of a given action potential, interpretation of $\dot{V}_{max}$ measured in multicellular tissues in terms of I_{Na} is complex. Studies of changes in $\dot{V}_{max}$ in more uniformly depolarized tissues or single cells under appropriate ionic conditions can yield convenient, albeit nonquantitative, indexes of changes in I_{Na}. Because action potential experiments study sodium channel properties under more physiological conditions, they provide a bridge between detailed studies of sodium channel properties and cell behavior.

Single Channel Behavior Underlying I_{Na} and $\dot{V}_{max}$

The concept of sodium channel availability used in these experiments derives from voltage-clamp experiments and the model of Hodgkin and Huxley. The Hodgkin-Huxley equations have been valuable for modeling the upstroke of the action potential and helpful for understanding excitability. However, evidence from single channel studies is persuasive that the Hodgkin-Huxley formalism does not accurately model sodium channel behavior.[23–25] To understand why $\dot{V}_{max}$ and I_{Na} are different, it is important to consider the single channel behavior that determines peak I_{Na} in the two measures. The time course of I_{Na} is determined primarily by the product of the time-to-opening (latency) of the channels and the mean open time. The magnitude of I_{Na} is the result of four factors: 1) the fraction of channels available for opening at the onset of the voltage step, often represented as h; 2) the fraction of those channels that open (versus those inactivating without opening); 3) the synchrony of opening; and 4) the single channel current. During voltage-dependent sodium channel protocols, voltage clamp steps keep the latter three factors constant, even though the number of channels that open at peak I_{Na} is only a fraction of the total.[12,26] On the other hand, during the upstroke of an action potential the membrane potential changes while sodium channels are activating. When the upstroke is slow, the fraction of available sodium channels contributing to $\dot{V}_{max}$ does not remain constant. During a rapid upstroke, many channels never contribute to $\dot{V}_{max}$ because it occurs before they can open. No model incorporating single channel behavior is yet available to calculate the upstroke of the action potential, but when developed, such a model should help us understand the complex sodium channel events that underlie the upstroke of the action potential.

References

1. Weidmann S: The effect of the cardiac membrane potential on the rapid availability of the sodium-carrying system. *J Physiol* (Lond) 1955;127:213–224
2. Hondeghem LM, Katzung BG: Time- and voltage-dependent interactions of antiarrhythmic drugs with cardiac sodium channels. *Biochim Biophys Acta* 1977;472:373–398
3. Strichartz GR, Cohen I: $\dot{V}_{max}$ as a measure of $\bar{G}_{Na}$ in nerve and cardiac membranes. *Biophys J* 1978;23:153–156
4. Cohen IS, Attwell D, Strichartz G: The dependence of the maximum rate of rise of the action potential upstroke on membrane properties. *Proc R Soc Lond* 1981;B214:85–86
5. Cohen CJ, Bean BP, Tsien RW: Maximal upstroke velocity ($\dot{V}_{max}$) as an index of available sodium conductance: Comparison of $\dot{V}_{max}$ and voltage clamp measurements of I_{Na} in rabbit Purkinje fibers. *Circ Res* 1984;54:636–651
6. Hondeghem L: Letter to the editor. *Circ Res* 1985;57:192–193
7. Courtney KR: Letter to the editor. *Circ Res* 1985;57:194–195
8. Fozzard HA, Hanck DA, Sheets MF: Non-linear relationship of maximal upstroke velocity to the sodium current in single canine cardiac Purkinje cells (abstract). *J Physiol* 1986;382:103P
9. Sheets MF, Hanck DA, Fozzard HA: Quinidine alters the relationship of $\dot{V}_{max}$ to Na current in single cardiac Purkinje cells (abstract). *Circulation* 1987;76(suppl IV):IV-149
10. Sheets MF, January CT, Fozzard HA: Isolation and characterization of single canine Purkinje cells. *Circ Res* 1983; 53:544–548
11. Oxford GS: Some kinetic and steady-state properties of sodium channels after removal of inactivation. *J Gen Physiol* 1981;77:1–22
12. Makielski JC, Sheets MF, Hanck DA, January CT, Fozzard HA: Sodium current in voltage clamped internally perfused canine cardiac Purkinje cells. *Biophys J* 1987;52:1–11
13. Provencher SW: A Fourier method for the analysis of exponential decay curves. *Biophys J* 1976;16:27–41
14. Hondeghem L, Katzung BG: Test of a model of antiarrhythmic drug action: Effects of quinidine and lidocaine on myocardial conduction. *Circulation* 1980;61:1217–1224
15. Gettes LS, Reuter H: Slow recovery from inactivation of inward currents in mammalian myocardial fibres. *J Physiol* (Lond) 1974;240:703–724
16. Chen C, Gettes LS, Katzung BG: Effect of lidocaine and quinidine on steady-state characteristics and recovery kinetics of $(dV/dt)_{max}$ in guinea pig ventricular myocardium. *Circ Res* 1975;37:20–29
17. Walton MK, Fozzard FA: The conducted action potential: Models and comparison to experiments. *Biophys J* 1983; 44:9–26
18. Fozzard HA, Friedlander I, Hanck DA, January JC, Makielski JC, Sheets MF: Sodium currents in single cardiac Purkinje cells. *J Am Coll Cardiol* 1986;8:79A–85A
19. Fozzard HA: Membrane capacity of the cardiac Purkinje fibre. *J Physiol* (Lond) 1966;182:255–264
20. Carmeliet EE, Willems J: The frequency dependent character of the membrane capacity in cardiac Purkinje fibres. *J Physiol* (Lond) 1971;213:85–93
21. Colastsky TJ: Mechanisms of action of lidocaine and quinidine on action potential duration in rabbit cardiac Purkinje fibers. An effect on steady state sodium currents? *Circ Res* 1982;50:17–27
22. Weld FM, Coromilas J, Rottman JN, Bigger JT Jr: Mechanisms of quinidine-induced depression of maximum upstroke

velocity in ovine cardiac Purkinje fibers. *Circ Res* 1982; 50:369–376
23. French RJ, Horn R: Sodium channel gating: Models, mimics and modifiers. *J Ann Rev Biophys Bioeng* 1983;12:319–356
24. Aldrich RW, Corey DP, Stevens CF: A reinterpretation of mammalian sodium channel gating based on single channel recordings. *Nature* 1983;306:436–441
25. Horn R, Vandenberg CA: Statistical properties of single sodium channels. *J Gen Physiol* 1984;84:505–534
26. Bean BP: Sodium channel activation in the crayfish giant axon. Must channels open before inactivating? *Biophys J* 1981;35:595–614

KEY WORDS • $\dot{V}_{max}$ • voltage clamp • sodium current • Purkinje cell • tetrodotoxin • quinidine